IEEE Access
Multidisciplinary | Rapid Review | Open Access Journal

Received April 9, 2018, accepted May 5, 2018, date of publication May 15, 2018, date of current version June 29, 2018.

Digital Object Identifier 10.1109/ACCESS.2018.2836348

Dynamic Modeling and Adaptive Sliding Mode Control for a Maglev Train System Based on a Magnetic Flux Observer

JUNQI XU[1,2], YOUGANG SUN[2,4], DINGGANG GAO[2,3], WEIHUA MA[3], SHIHUI LUO[3], AND QINGQUAN QIAN[1]

[1]School of Electrical Engineering, Southwest Jiaotong University, Chengdu 610031, China
[2]Maglev Transportation Engineering R&D Center, Tongji University, Shanghai 201804, China
[3]Traction Power State Key Laboratory, Southwest Jiaotong University, Chengdu 610031, China
[4]College of Logistics Engineering, Shanghai Maritime University, Shanghai 200135, China

Corresponding author: Yougang Sun (ygsun@shmtu.edu.cn)

This work was supported in part by the National Key Research and Development Program of China, Research on Key Technologies of Maglev Transportation System, under Grant 2016YFB1200600, and in part by the Fundamental Research Funds for the Central Universities.

ABSTRACT The control method and dynamic performance of a magnetic suspension system, which is the core component of maglev trains, have a significant influence on the performance of the maglev train. Currently, a control strategy based on the current feedback is widely used. However, the stable range of control parameters is relatively small, making it difficult to identify stable regions for the control parameters. In addition, the strong interactions between the control parameters are cause issues in the control. In this paper, a control strategy based on the flux density observer is proposed using an analysis of the working principle and the structure of the suspension system. A nonlinear dynamic model of a maglev system is established by utilizing the state equation of the flux feedback. Based on the current and voltage feedback, a hybrid magnetic flux density observer is presented. According to the mathematical model, an adaptive sliding mode controller is designed to reduce the upper bound of both uncertainty and interference of the sliding mode controller. Finally, a theoretical analysis and the effectiveness of the proposed control strategy are verified using both simulations and experiments.

INDEX TERMS Maglev system, dynamic model, flux observer, adaptive control, sliding mode control.

I. INTRODUCTION

The magnetic suspension system is widely applied in many fields, such as maglev trains [1]–[3], magnetic bearings [4], magnetic suspension sliders [5], and magnetic suspension precision platforms [6]. Maglev trains have attracted wide attention of researchers because of their unique advantages, such as contactless motion, comfortability and being environmentally friendly.

Stable suspension is the key to the contactless operation of the maglev train. The current research focus on the magnetic suspension control system is to reduce the debugging difficulty and to improve its robustness. The study of maglev control has led to a mainstream control scheme with a current loop as the inner loop and airgap loop as the outer loop. The scheme is convenient to debug and realize the maglev train operation. However, all of the state feedback is needed in the mainstream control scheme, which includes the suspension airgap, the velocity of the electromagnet, and the current in the electromagnetic coil. Liu and Chang [7] proposed a double loop control method. The current is used as one of the state feedbacks, and the magnetic suspension system is divided into the current loop and the position loop for control. The effectiveness of the control method is verified with a theoretical analysis and simulations using a linearized model. Luat and Kim [8] proposed the control of the MIMO (Multiple Input Multiple Output) maglev vehicle based on the SISO (Single Input Single Output) control method, which compensated for the rotational motions. However, some nonlinear terms were ignored in the mathematical model. Since the linear controller may cause the maglev train to vibrate under external disturbances [9], Zhou *et al.* [10], [11] studied the active control method and applied a tuned mass

damper (TMD) to the maglev girder, thereby achieving improved results. Sun *et al.* [12] proposed the repetitive learning control law to solve the problem of stable suspension under periodic disturbances. However, the robustness of the control method will be worse under the non-periodic disturbances, and the control algorithm uses current as the state feedback. Wai *et al.* [13] designed a self-adapted fuzzy-neural network controller for the magnetic suspension system with strong robustness. Xu *et al.* [14] proposed a robust control law to guarantee a magnitude limitation of the airgap for the magnetic suspension system. The feedback control states of the abovementioned literature usually include the airgap or the current of the electromagnetic coil. However, experiments show that it is difficult to obtain the control parameter values to stabilize the system when these state variables are used for the feedback. In addition, there are large interactions between the control parameters. In particular, when the inner loop (current loop) is debugged, the dynamic performance of the system is readily influenced by changes in the control parameters, which indicates that the anti-disturbance capabilities of the current-feedback method are poor. For the situation that needs strong robustness, the magnetic flux-loop is an excellent choice to be used as the inner loop instead of the current loop. The magnetic flux loop was introduced in 1976 [15] and was successfully applied to the magnetic levitation line at the Birmingham Airport. After 2000, Goodall [16] noted that although the magnetic flux sensors are not very convenient, the suspension control is easy to debug and has good robustness from using the flux feedback. Therefore, the method of using magnetic flux feedback instead of current feedback is the new choice for magnetic suspension systems.

As mentioned previously, most of the suspension control methods and dynamic characteristic analyses are based on linearized models, which are implemented in a very small neighborhood near the equilibrium point. Therefore, when the system deviates from the equilibrium point, the linearized model becomes invalid. Whether the system can continue to use the linearized model when the suspension state deviates far away from the equilibrium point requires further consideration. In addition, various control algorithms derived from the flux feedback method need to be studied further. With the development of nonlinear science and modern control theory, advanced control algorithms, such as the optimal control, fuzzy control, adaptive control and sliding mode variable structure control, have achieved success in many fields. However, these algorithms are not widely used in the field of magnetic suspension systems. Combining the advanced control algorithm with the flux feedback control scheme to design a suspension controller with high stability and robustness is a problem that deserves further study. Finally, although the use of the magnetic flux as a state feedback has obvious advantages, the hall devices or fluxmeters in the current market are either not suitable for the measuring range or cannot be installed properly. Moreover, the measurements are relatively rough, and the calibration of the sensors is not accurate. Maglev trains that already operate would also need to cut each coil to embed the magnetic flux sensors, which is not practical. Thus, obtaining the magnetic flux without damaging the current coil structure is difficult.

In this paper, we aim at solving the problem mentioned above. Initially, we derive a nonlinear dynamic model of the magnetic suspension system based on the magnetic flux density feedback. Then, a hybrid magnetic flux density observer is proposed to measure the required magnetic flux density state. Next, we design an adaptive sliding mode controller based on the magnetic flux density feedback without any linear processing. The stability of the designed closed-loop system is proven using Lyapunov techniques. Simulation and experimental results are included to demonstrate that the presented control strategy is effective.

The paper is arranged as follows. In Section II, the dynamical models for the maglev system are explicitly provided based on the flux feedback. The hybrid magnetic flux density observer development is presented in Section III. The main results, including the controller design and closed-loop stability analysis, are included in Section IV. Simulation results are provided in Section V, and hardware experimental results are included in Section VI. Finally, the study's conclusions are provided in Section VII.

II. DYNAMICS MODEL OF MAGLEV SYSTEM BASED ON FLUX FEEDBACK

Based on the mechanical structure of maglev trains, there are 4∼5 bogies in a given carriage, each having 4 suspending points. The experiment for the four electromagnetic suspension modules is implemented [17], which demonstrates that the multiple electromagnets suspension control system can be deformalized into a single-electromagnet control system, as shown in Fig. 1. The single-electromagnet control system includes the suspension electromagnet, suspension controller, maglev rail, power supply and sensor. Through reasonable simplification, the schematic diagram of a single point suspension system is illustrated in Fig. 2. The $F(B, z)$ is the electromagnetic force, which is produced from the suspension electromagnet, $z(t)$ is the airgap between the suspension electromagnet and the maglev rail, $i(t)$ is the coil current of

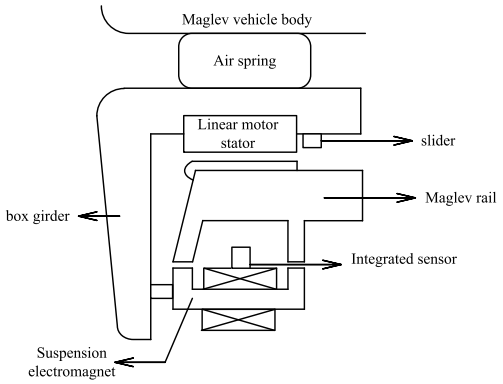

FIGURE 1. Magnetic suspension control system.

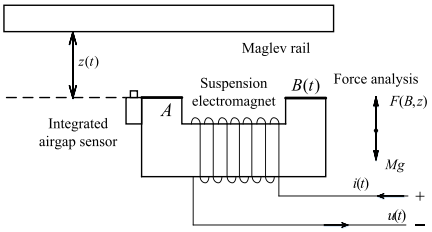

FIGURE 2. The single-electromagnet system.

the suspension electromagnet, $u(t)$ is the excitation voltage at both ends of the suspension electromagnet coil, $B(t)$ is the magnetic flux density at the suspension electromagnet surface, and A is the pole area of the suspension electromagnet. Assuming that the suspension electromagnet and maglev rail are rigid bodies, the suspension system has only the vertical degree of freedom, which is a single degree of freedom system.

The absolute reference frame is used as the standard where downward is the positive direction and upward is the negative direction [18]–[20]. Based on the fundamental knowledge of electromagnetics, the airgap flux of the suspension electromagnet, which neglects the magnetic flux leakage, can be written as follows:

$$\phi_m \approx \phi_T = \frac{F_m}{R_m} = \frac{Ni(t)}{2z(t)/(\mu_0 A)} \tag{1}$$

where F_m is the magnetic potential, R_m is the reluctance, ϕ_m is the total flux, and ϕ_T is the principal flux.

The airgap magnetic flux density of the suspension electromagnet is as follows:

$$B = \frac{\mu_0 Ni(t)}{2z(t)} \tag{2}$$

The expression of the electromagnetic force of the suspension electromagnet can be obtained as

$$\begin{aligned} F &= \frac{dW_m}{dz} = \frac{d}{dz}\int w_m dv = \frac{d}{dz}\left(\frac{1}{2}BHV\right) \\ &= \frac{d}{dz}\left(\frac{B^2 Az}{\mu_0}\right) = \frac{B^2 A}{\mu_0} \end{aligned} \tag{3}$$

where w_m is the energy density of the magnetic field, and W_m is the magnetic field energy within the volume V.

The control voltage equation of the suspension electromagnet can be obtained as follows:

$$u(t) = Ri(t) + \frac{d\Psi}{dt} \approx \frac{d}{dt}(N\phi_r) = Ri(t) + NA\frac{dB}{dt} \tag{4}$$

where Ψ is the airgap flux linkage.

Using Newton's second law [28]–[30], the dynamics equation of the suspension system can be expressed as

$$M\ddot{z}(t) = -F(t) + Mg \tag{5}$$

The nonlinear model of the magnetic suspension system is therefore

$$\begin{cases} B(t) = \dfrac{\mu_0 Ni(t)}{2z(t)} \\ F(t) = \dfrac{B^2(t)A}{\mu_0} \\ M\ddot{z}(t) = -F(t) + Mg \\ u(t) = \dfrac{2Rz(t)}{\mu_0 N}B(t) + NAB(t) \end{cases} \tag{6}$$

where μ_0 is the vacuum permeability, N is the coil number, R is the electromagnet internal resistance, and g is the gravitational acceleration.

For the suspension system, $\mathbf{x} = [x_1\ x_2\ x_3]^T = [z\ \dot{z}\ B]^T$ is selected as the system state variable, and the relationship between the state variables is expressed as follows:

$$\begin{cases} \dot{x}_1 = x_2 \\ \dot{x}_1 = g - \dfrac{A}{\mu_0 M}x_3^2 \\ \dot{x}_3 = -\dfrac{2R}{\mu_0 AN^2}x_1 x_3 + \frac{1}{NA}u \end{cases} \tag{7}$$

The nonlinear state space equation of the suspension system can be expressed as

$$\begin{cases} \dot{x} = f(x) + g(x)u \\ y = h(x) \end{cases} \tag{8}$$

where

$$f(x) = \begin{bmatrix} x_2 \\ g - \frac{S}{\mu_0 M}x_3^2 \\ -\frac{2R}{\mu_0 N^2}x_1 x_3 \end{bmatrix}, \quad g(x) = \begin{bmatrix} 0 \\ 0 \\ \frac{1}{NS} \end{bmatrix},$$
$$h(x) = x_1, \quad u = u(t)$$

III. HYBRID MAGNETIC FLUX DENSITY OBSERVER

The accuracy of the magnetic flux density obtained from the flux density observer method depends primarily on the mathematic model of the observer. The two existing flux observer models are those for voltage and current.

Without considering the reluctance of the stator core and the influence of the airgap change on the inductance of the electromagnetic coil, the airgap flux density in the current model can be expressed as

$$B_i(t) = \frac{\mu_0 Ni(t)}{2z(t)} \tag{9}$$

The airgap flux density in the voltage model can be formed as

$$B_u(t) = \frac{1}{AN}\int (u(t) - Ri(t))dt \tag{10}$$

The frequency-domain formulas of the two models can be expressed as

$$\mathrm{B}_i(s) = \mu_0 NI(s)/2Z(s) \tag{11}$$

$$\mathrm{B}_u(s) = \frac{1}{AN}(U(s) - RI(s)) \tag{12}$$

The current model is more accurate at low frequencies or static times, but the error is very large at high frequencies. The voltage model is more accurate at higher frequency. However, due to using of the pure integration element, the small DC bias will eventually lead to integral saturation, so the voltage model has a large error at low frequencies. Based on these reasons, a hybrid observer model is presented that combines the current model and the voltage model. The voltage model works at the high frequencies, and a high pass filter can be used to remove the observed value of the current model. In the low frequency situation, the current model is preferred, and the observation value of the voltage model is removed through a low pass filter. The model combines the advantages of the current and voltage models and can measure the flux of the full frequency section more accurately.

The airgap flux density in the low frequency situation is as follows:

$$\mathrm{B}_{LF}(s) = \frac{1}{s\tau_{LF}+1} B_i(s) = \frac{K_{LF}}{s\tau_{LF}+1} I(s) \tag{13}$$

where $K_{LF} = \mu_0 NA/2z$, and τ_{LF} is the low pass filter time constant.

The airgap flux density at high frequencies $\Phi_{HF}(s)$ is written as follows:

$$B_{HF}(s) = \frac{\tau_{HF} s}{s\tau_{HF}+1} B_u(s) = \frac{K_{HF}}{(s\tau_{HF}+1)N} [U(s) - RI(s)] \tag{14}$$

where $K_{HF} = \tau_{HF}$, and τ_{HF} is the high pass filter time constant.

When $\tau_{HF} = \tau_{LF} = \tau$, the airgap flux in the full band $\Phi(s)$ can be written as

$$\mathrm{B}(s) = \mathrm{B}_{LF}(s) + \mathrm{B}_{HF}(s) = \frac{1}{s\tau+1}\mathrm{B}_i(s) + \frac{s\tau}{s\tau+1}\mathrm{B}_u(s) \tag{15}$$

The proposed observer model can accurately observe the flux density. This overcomes the problem that the current model is not accurate at high frequencies and the voltage model is not accurate in low frequencies.

IV. DESIGN OF AN ADAPTIVE SLIDING MODE CONTROL

This section will provide the process of the adaptive nonlinear sliding mode controller design for the magnetic suspension system based on the flux density feedback. The analysis for the stability of the closed-loop system using the Lyapunov method does not assume any linear approximations. To facilitate the latter design, the system error is defined as follows [31]–[34]:

$$e_1 = x_1 - x_{1d} \tag{16}$$

$$e_2 = x_2 - x_{2d} \tag{17}$$

Based on the nonlinear system model (7), a novel sliding mode surface is proposed as:

$$S = \lambda_1 e_1 + \lambda_2 e_2 + g - \frac{A}{\mu_0 M} x_3^2 \tag{18}$$

$$\dot{S} = \lambda_1 e_2 + \lambda_2 (g - \frac{A}{\mu_0 M} x_3^2) + \frac{4R}{\mu_0 M N^2} x_1 x_3^2 - \frac{2x_3}{\mu_0 M N} u \tag{19}$$

where $\lambda_1, \lambda_2 \in \mathbb{R}^+$ are positive constants.

The adaptive sliding mode control law based on the flux density feedback is presented as

$$u = \frac{\mu_0 M N}{2x_3} \left(\frac{4Rx_1 x_3^2}{\mu_0^2 M N^2} + \lambda_2 (g - \frac{Ax_3^2}{\mu_0 M}) + \lambda_1 e_2 + \hat{w}\,\mathrm{sign}(S) \right) \tag{20}$$

where $\hat{w}$ is the adjustable estimated value of w, x_3 is the flux density feedback, which can be obtained from the flux density observer (15), sign$(\cdot)$ is the signum function, and S denotes the dynamic sliding surface defined by (18).

The adaptive laws of $\hat{w}$ are proposed as

$$\dot{\hat{w}} = \frac{1}{\alpha} |S| \tag{21}$$

where $\alpha \in \mathbb{R}^+$ denotes the adaptive gain. The estimation error is defined as:

$$\tilde{w}(t) = \hat{w}(t) - w(t) \tag{22}$$

The estimation velocity of $\hat{w}$ can be adjusted using α. Choosing a suitable adaptive gain α can effectively reduce the chattering phenomenon. The validity of the adaptive algorithm will be proven using Lyapunov theory.

Theorem 1: The nonlinear dynamic sliding surface (18) and proposed controller (20) with an adaptive law (21) guarantee that $\hat{w}$ has an upper bound. That is, there exists a constant $w_d \in \mathbb{R}^+$, that satisfies: $\forall t > 0, \hat{w}(t) \le w_d$.

Proof: Initially, a Lyapunov function is chosen as:

$$V_w = \frac{1}{2} s^2 + \frac{1}{2} \alpha \tilde{w}^2 \tag{23}$$

Taking the time derivative of V_w, one can derive the following result:

$$\begin{aligned}
\dot{V}_w &= s\dot{s} + \alpha \tilde{w}\dot{\tilde{w}} \\
&= s\left(\lambda_1 e_2 + \lambda_2 (g - \frac{A}{\mu_0 M} x_3^2) + \frac{4R}{\mu_0 M N^2} x_1 x_3^2 \right. \\
&\quad \left. - \frac{2x_3}{\mu_0 M N} u \right) + \alpha \left(\hat{w} - w \right) \frac{1}{\alpha} |s| \\
&= \mathrm{s}\left(\lambda_2 (g - \frac{A}{\mu_0 M} x_3^2) \right. \\
&\quad - \frac{2x_3}{\mu_0 M N} \left(\frac{\mu_0 M N}{2x_3} \left(\frac{4Rx_1 x_3^2}{\mu_0^2 M N^2} + \lambda_1 e_2 \right. \right. \\
&\quad \left. \left. + \lambda_2 (g - \frac{Ax_3^2}{\mu_0 M}) \right) \right) + \frac{4R}{\mu_0 M N^2} x_1 x_3^2 + \lambda_1 e_2 \Big) \\
&\quad + \alpha \left(\hat{w} - w \right) \frac{1}{\alpha} |s| \\
&= -\mathrm{s}\, \hat{w}\mathrm{sign}\,(s) + \left(\hat{w} - w \right) |s| \\
&\le -\hat{w} |s| + \hat{w} |s| - w |s| \\
&\le -w |s| \le 0
\end{aligned} \tag{24}$$

According to the Lyapunov stability theory [21], [22], $\hat{w}$ is bounded. Thus, there exists a constant $w_d \in \mathbb{R}^+$ such that $\forall t > 0, \hat{w}(t) \leq w_d$. QED.

Theorem 2: The proposed adaptive sliding mode control law (20), along with the adaptive law (21), can drive the error of the airgap to be zero in a finite amount of time.

Proof: To prove the conclusion of Theorem 2, we define a Lyapunov function candidate $V_1 \in \mathbb{R}^+$ as follows:

$$V_1 = \frac{1}{2}s^2 + \frac{1}{2}\alpha_1(\hat{w} - w_d)^2 \tag{25}$$

Taking the time derivative of V_1, one can derive the following result:

$$\begin{aligned}\dot{V}_1 &= s\dot{s} + \alpha_1(\hat{w} - w_d)\dot{\hat{w}} \\ &= s\left(\lambda_1 e_2 + \lambda_2(g - \frac{A}{\mu_0 M}x_3^2) + \frac{4R}{\mu_0 MN^2}x_1x_3^2 \right. \\ &\quad \left. -\frac{2x_3}{\mu_0 MN}u\right) + \alpha_1(\hat{w} - w_d)\frac{1}{\alpha}|s|\end{aligned} \tag{26}$$

Substituting proposed control law (20) into (26), the following can be developed:

$$\begin{aligned}\dot{V}_1 &= \mathrm{s}(\lambda_1 e_2 + \left(-\frac{2x_3}{\mu_0 MN}\left(\frac{\mu_0 MN}{2x_3}\left(\frac{4Rx_1x_3^2}{\mu_0^2 MN^2}\right.\right.\right. \\ &\quad \left.\left.\left. +\lambda_1 e_2 + \hat{w}\mathrm{sign}\,(S) + \lambda_2(g - \frac{Ax_3^2}{\mu_0 M})\right)\right)\right) \\ &\quad + \frac{4R}{\mu_0 MN^2}x_1x_3^2 + \lambda_2(g - \frac{A}{\mu_0 M}x_3^2)) \\ &\quad + \alpha_1(\hat{w} - w_d)\frac{1}{\alpha}|s| \\ &= \mathrm{s}\left(-\hat{w}\mathrm{sign}\,(s)\right) + \frac{\alpha_1}{\alpha}|s|\left(\hat{w} - w_d\right) \\ &= -|s|\,\hat{w} + \frac{\alpha_1}{\alpha}|s|\left(\hat{w} - w_d\right) \\ &= -\sqrt{2}\hat{w}\frac{|s|}{\sqrt{2}} + \sqrt{2}\frac{\alpha_1}{\alpha}|s|\frac{\left(\hat{w} - w_d\right)}{\sqrt{2}} \\ &\leq -\sqrt{2}\hat{w}\frac{|s|}{\sqrt{2}} - \sqrt{2}\frac{\alpha_1}{\alpha}|s|\frac{\left|\hat{w} - w_d\right|}{\sqrt{2}}\end{aligned} \tag{27}$$

Define $\beta_1 = \hat{w}$ and $\beta_2 = \frac{\sqrt{\alpha_1}}{\alpha}|s|$. Therefore, (27) can be updated as follows:

$$\begin{aligned}\dot{V}_1 &\leq -\min\left(\sqrt{2}\beta_1, \sqrt{2}\beta_2\right)\left(\frac{|s|}{\sqrt{2}} + \sqrt{\alpha_1}\frac{\left|\hat{w} - w_d\right|}{\sqrt{2}}\right) \\ &\leq -\min\left(\sqrt{2}\beta_1, \sqrt{2}\beta_2\right)\sqrt{\left(\frac{|s|}{\sqrt{2}}\right)^2 + \left(\sqrt{\alpha_1}\frac{\left|\hat{w} - w_d\right|}{\sqrt{2}}\right)^2} \\ &= -\beta V_1^{\frac{1}{2}}\end{aligned} \tag{28}$$

where $\beta = \min\left(\sqrt{2}\beta_1, \sqrt{2}\beta_2\right)$. Therefore, using [23, Th. 4.2], the system can converge to the sliding mode surface $S = 0$ in a finite time. In other words, the system with the proposed control law is stable. QED.

V. SIMULATION RESULTS

The parameters of the magnetic suspension system are based on the test maglev train at the national maglev center of Tongji University and are shown in Table 1. The initial position of the suspension airgap is 0.016 m, and the target position of the airgap is 0.008 m. The MATLAB/SIMULINK platform is utilized to simulate the adaptive sliding mode control (ASMC(B)) based on the flux density observer, which is used for comparison with both the traditional linear PID [24], [25] and the sliding mode controller (SMC(i))[26], which are based on the current feedback. The ASMC(B) controller parameters are sufficiently tuned using a trial-and-error method to obtain the best performance, which yields the following values: $\lambda_1 = 1200$, $\lambda_2 = 200$, and $\alpha = 0.015$.

TABLE 1. Physical parameter values.

Symbol & Value
$M = 700kg$
$A_m = 0.024m^2$
$N_m = 450$
$R_m = 1.2\Omega$
$\mu_0 = 4\pi \times 10^{-7}\, H \cdot m^{-1}$
$x_{10} = 0.016m$
$\eta = 0$
$x_{1d} = 0.008m$

A. STATIONARY SUSPENSION (STEP RESPONSE)

Under the action of ASMC(B), linear PID and SMC (i), the dynamic response of the airgap is shown in Fig. 3.

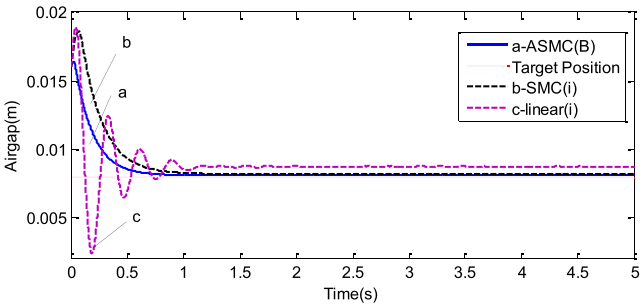

FIGURE 3. Airgap dynamic response.

As shown in Fig. 3, the airgap trajectory of the ASMC(B) converges rapidly to the target position ($x_{1d} = 0.008m$) within a finite time without overshoot. However, the conventional linear controller allows the trajectory to converge on the target position, but the dynamic performance is poor, and the steady-state error is larger with an obvious overshoot. The performance of SMC (i) based on current is similar to that of ASMC(B) without disturbance, but the dynamic performance is slightly worse than that of the ASMC(B) and requires more time to reach the dynamic sliding surface $S = 0$.

The phase locus under the ASMC(B) is shown in Fig. 4. The state of the system reaches the sliding surface quickly from the starting point, and then moves along the sliding surface to the target position with a smooth phase trajectory. The flux density obtained from the flux density observer is shown in Fig. 5. It is shown that the observer can effectively measure the flux density of the system. The change in the adaptive gain $\hat{w}$ in the ASMC is shown in Fig. 6. It can be seen that $\hat{w}$ can converge to a positive constant in a finite time. The simulation results prove the theoretical analysis that $\hat{w}$ is bounded.

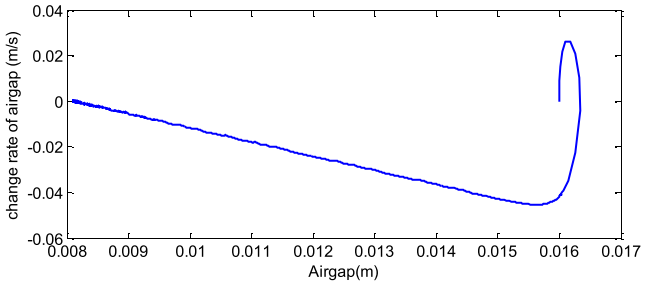

FIGURE 4. Phase locus.

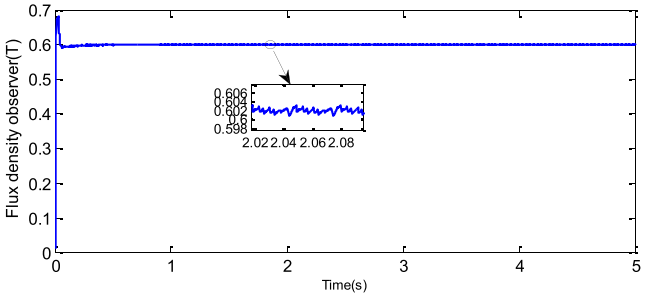

FIGURE 5. Flux density observer.

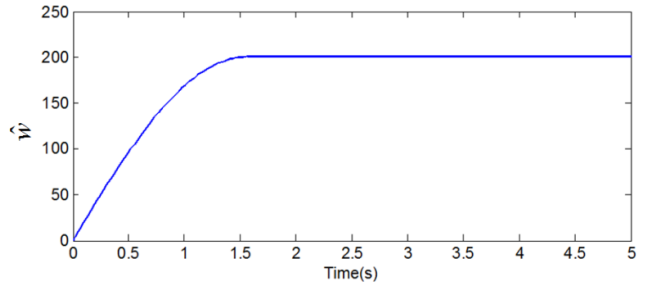

FIGURE 6. Adaptive gain $\hat{w}$.

We can learn from the simulation results of the stationary suspension that the ASMC(B) is better than linear PID and SMC(i) in both dynamic and steady-state performances. The phase locus under the ASMC(B) is relatively smooth. Fig. 5 shows that the flux density observer can work effectively. We can learn from Fig. 6 that the adaptive gain $\hat{w}$ can be adjusted adaptively. To summarize, when the train is suspended statically, the ASMC(B) can work efficiently.

B. DYNAMIC RESPONSE WITH DISTURBANCE

It is inevitable that the maglev train will be affected from disturbance forces. According to the disturbance force amplitude of [26], we add an external disturbance force $f_d = 1400\sin(10 \cdot t)$ to the system, as shown in Fig. 7. The simulation results compare the dynamic responses of the ASMC(B) and SMC (i).

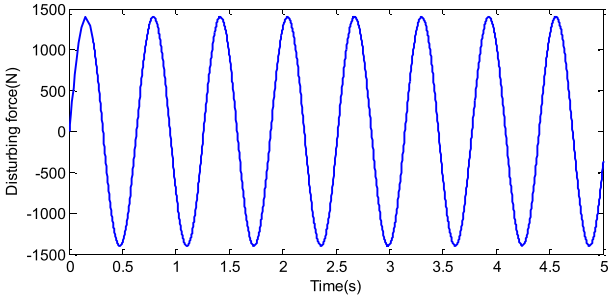

FIGURE 7. Disturbance force.

The simulation results of the airgap dynamic response are shown in Fig. 8. Under a continuous disturbance, both the ASMC(B) and SMC (i) show the airgap state reaches the target position and maintains its stability. However, the ASMC(B) reaches the sliding surface $S = 0$ more quickly and more accurately than the SMC (i). In the ASMC(B), the airgap fluctuation is obviously lower than that of SMC (i), giving it a stronger robustness. This indicates that the closed-loop stiffness of the magnetic suspension system based on the flux density control is larger than that of the current controlled maglev system, which is consistent with the theoretical analysis.

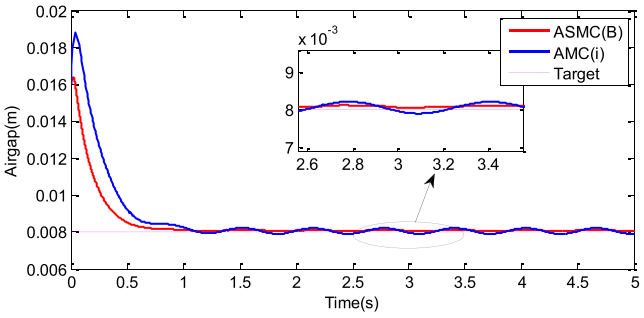

FIGURE 8. Airgap dynamic response under the disturbance.

The simulation result of the linear PID controller under the continuous disturbance shown in Fig. 7 based on the flux feedback is shown in Fig. 9. We can learn from Fig. 9 that the system is unstable with the linear PID controller under the disturbance, whose maximum acceleration is twice the gravitational acceleration, which is consistent with the experimental results. In the experiment, the linear controller can be destabilized under the disturbance by more than approximately 1.5 times the gravitational acceleration. However, the proposed nonlinear controller in this paper can achieve self-stabilization suspension under the same disturbance

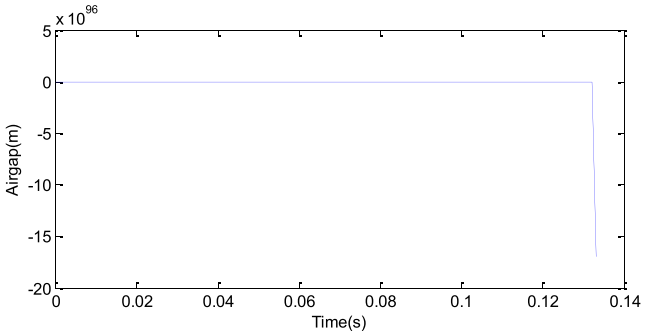

FIGURE 9. Airgap dynamic response under the disturbance with PID(B).

force. This demonstrates that the ASMC(B) is more efficient and robust. The phase locus under the continuous disturbance is shown in Fig. 10. Due to the existing disturbance, the trajectory fluctuates. However, it is stable over a certain range of circles, which is consistent with the Lyapunov sense of stability. It is demonstrated in Fig. 11 that the flux density can be effectively measured using the proposed flux density observer of (15).

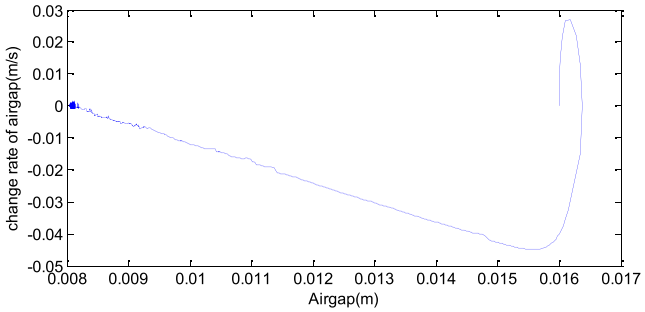

FIGURE 10. Phase locus with the ASMC(B).

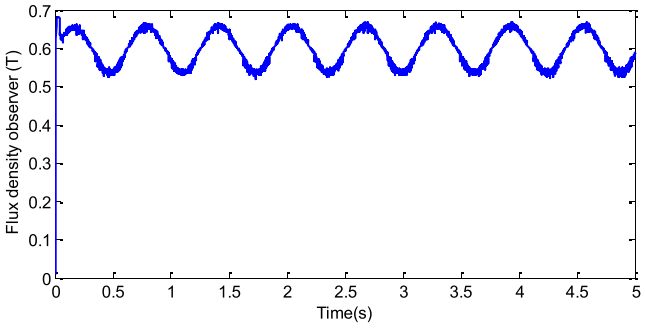

FIGURE 11. Flux density observer under the disturbance.

It is shown in Figs. 8-11 that the proposed ASMC(B) has better anti-disturbance capabilities than the linear PID and SMC(i) approaches. It can be seen from the phase locus that the system is stable in the sense of the Lyapunov stability, and the flux density observer can work effectively. In conclusion, the simulation results demonstrate the effectiveness of the proposed nonlinear control strategy with the flux density observer.

VI. PRELIMINARY EXPERIMENTAL RESULTS

After the numerical simulations, significant effort are made to implement the experiments with the aim of examining the practical performance of the proposed control scheme. The experiments are implemented in the national low-speed maglev test line. The full-scale test maglev train and maglev experimental line are shown in Fig. 12, and the signal transduction is illustrated in Fig. 13. In the test maglev vehicle, the maglev train is stably suspended from the interaction between the digital controller and the flux density observer.

FIGURE 12. Experimental platform of the maglev train.

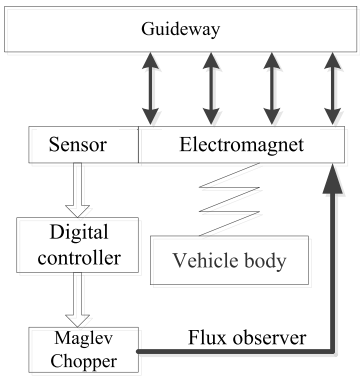

FIGURE 13. Signal transmission in the test maglev vehicle.

The sampling frequency is 2500 Hz, and the experimental parameters of the system and the parameters of the ASMC(B) are consistent with the parameters used in the theoretical analysis and simulation. The maglev train completes a dynamic process through running and stationary suspension. The speed of the test maglev train is provided as Fig. 10, which shows that 0 s - 490 s is the running process whose maximum speed is approximately 100 km/h. From 490 s–530 s is the static process (stationary suspension). The train runs again from 530 s–1150 s whose maximum speed is approximately 100 km/h. The airgap response and flux density of the observer are shown in Figs. 11-12.

It can be observed from Figs. 14-16 that in the stage of stationary suspension, the airgap is in the target position of 8 mm, and the curve is stable and smooth. The flux density is also stable during the stationary suspension stage at approximately 0.6 T. However, when the train is running,

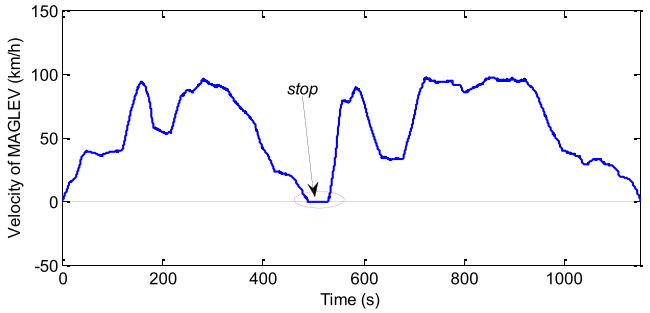

FIGURE 14. Experimental results: the speed of the train.

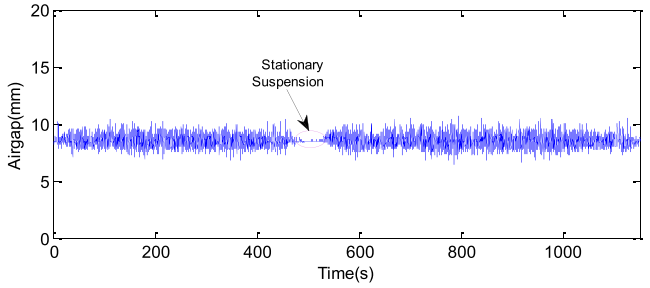

FIGURE 15. Experimental results: suspension airgap response.

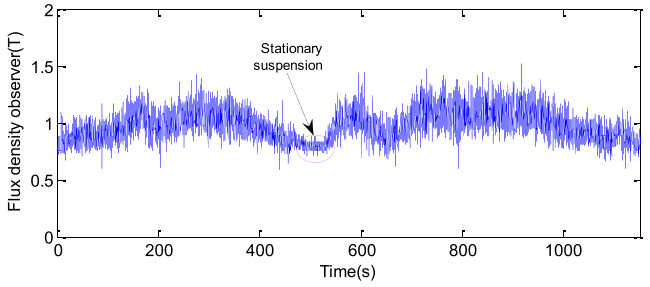

FIGURE 16. Experimental results: flux density.

the airgap fluctuates from 6.5 mm to 10.5 mm, which is caused by the rail gap (seam between the two rails). When the speed of the train increases, the flux density becomes larger. This is because higher speeds cause faster changes in the rail gap, which results in a more complex disturbance. Moreover, considering the aerodynamic effects, the higher speed can also result in a larger aerodynamic lift and down force [27], which also requires increased flux density to improve the robustness. However, the disturbances caused from various speeds is different, and the airgap response of the running test maglev train can be consistent under the proposed control strategy. The facts mentioned above prove that the AMSC(B) is an effective method with a stronger robustness.

VII. CONCLUSIONS

In this paper, a nonlinear dynamic model of magnetic suspension based on the flux density feedback is established. A hybrid magnetic flux density observer with a mixed current and voltage is proposed to overcome the difficulty of installing the magnetic flux sensor. Next, this observer is combined with the adaptive sliding mode controller to reduce the requirements on the upper bound of the uncertainty and disturbance and improves the stiffness of the suspension system. The simulation results show that if this control method is adopted, the parameter stability area increases and the control parameters, which satisfy the system dynamic performance, can be easily obtained. Moreover, the influence of the control parameters on the system dynamic performance is not obvious. For external disturbances, the controller has a better robustness than the current feedback sliding mode controller, and the controller is easier to implement in the structure. Finally, the experimental results demonstrate that the presented control strategy significantly improves the robustness and dynamic performance. In our future work, we will attack the maglev vehicle-guideway interaction vibration problem in the turnout junction by utilizing the flux feedback method.

REFERENCES

[1] R.-J. Wai, K.-L. Chuang, and J.-D. Lee, "On-line supervisory control design for MagLev transportation system via total sliding-mode approach and particle swarm optimization," *IEEE Trans. Autom. Control*, vol. 55, no. 7, pp. 1544–1559, Jul. 2010.

[2] J. Li, J. Li, D. Zhou, P. Cui, L. Wang, and P. Yu, "The active control of MagLev stationary self-excited vibration with a virtual energy harvester," *IEEE Trans. Ind. Electron.*, vol. 62, no. 5, pp. 2942–2951, May 2015.

[3] D. F. Zhou, C. H. Hansen, and J. Li, "Suppression of MagLev vehicle–girder self-excited vibration using a virtual tuned mass damper," *J. Sound Vib.*, vol. 330, no. 5, pp. 883–901, Feb. 2011.

[4] D. Jung and H. DeSmidt, "A new hybrid observer based rotor imbalance vibration control via passive autobalancer and active bearing actuation," *J. Sound Vib.*, vol. 415, pp. 1–24, Feb. 2018.

[5] Y.-M. Kao, N.-C. Tsai, and H.-L. Chiu, "Five-DOF innovative linear MagLev slider to account for pitch, tilt and load uncertainty," *Mech. Syst. Signal Process.*, vol. 84, pp. 673–698, Feb. 2017.

[6] F. Xing, B. Kou, and L. Zhang, "Design of a control system for a MagLev planar motor based on two-dimension linear interpolation," *Energies*, vol. 10, no. 8, p. 1132, Aug. 2017.

[7] H.-K. Liu and W.-S. Chang, "Double-loop control of MagLev train," *Control Eng. China*, vol. 14, no. 2, pp. 198–200, Feb. 2007.

[8] T. H. Luat and Y.-T. Kim, "Design of a MIMO levitation controller for MagLev transportation system," *J. Adv. Comput. Intell. Intell. Inform.*, vol. 21, no. 4, pp. 591–596, Jul. 2017.

[9] D. Zhou, C. H. Hansen, J. Li, and W. Chang, "Review of coupled vibration problems in EMS MagLev vehicles," *Int. J. Acoust. Vib.*, vol. 15, no. 1, p. 10, Mar. 2010.

[10] D. Zhou, P. Yu, L. Wang, and J. Li, "An adaptive vibration control method to suppress the vibration of the MagLev train caused by track irregularities," *J. Sound Vib.*, vol. 408, pp. 331–350, Nov. 2017.

[11] D. Zhou, J. Li, and K. Zhang, "An adaptive control method to suppress the MagLev track-induced self-excited vibration," in *Proc. Int. Conf. Consum. Electron., Commun. Netw.*, Apr. 2011, pp. 4723–4727.

[12] Y. Sun, H. Qiang, X. Mei, and Y. Teng, "Modified repetitive learning control with unidirectional control input for uncertain nonlinear systems," in *Neural Computing and Applications*. 2017, pp. 1–10, doi: 10.1007/s00521-017-2983-y.

[13] R. J. Wai, M. W. Chen, and J. X. Yao, "Observer-based adaptive fuzzy-neural-network control for hybrid MagLev transportation system," *Neurocomputing*, vol. 175, pp. 10–24, Jan. 2016.

[14] J. Xu, Y.-H. Chen, and H. Guo, "Robust levitation control for MagLev systems with guaranteed bounded airgap," *ISA Trans.*, vol. 59, pp. 205–214, Nov. 2015.

[15] R. M. Goodall, "Suspension and guidance control system for a DC attraction MagLev vehicle," in *Proc. IEEE Conf. Publ.*, Sep. 1976, pp. 100–103.

[16] R. M. Goodall, "On the robustness of flux feedback control for electromagnetic MagLev controllers," in *Proc. MagLev*, Rio de Janeiro, Brazil, Jun. 2000, pp. 197–202.

[17] H. Qiang, W. Li, Y. Sun, and X. Liu, "Levitation chassis dynamic analysis and robust position control for MagLev vehicles under nonlinear periodic disturbance," *J. Vibroeng.*, vol. 19, no. 2, pp. 1273–1286, Mar. 2017.
[18] Y. G. Sun, H. Y. Qiang, J. Q. Xu, and D. S. Dong, "The nonlinear dynamics and anti-sway tracking control for offshore container crane on a mobile harbor," *J. Mar. Sci. Technol.-Taiwan*, vol. 25, no. 6, pp. 656–665, Dec. 2017.
[19] N. Sun, Y. Wu, Y. Fang, and H. Chen, "Nonlinear antiswing control for crane systems with double-pendulum swing effects and uncertain parameters: Design and experiments," *IEEE Trans. Automat. Sci. Eng.*, to be published.
[20] Y. Sun, H. Qiang, D. Chang, and R. Wang, "Response characteristic analysis of nonlinear vortex-induced vibration of tension leg platform in deep sea," *J. Balkan Tribol. Assoc.*, vol. 22, no. 3, pp. 2518–2534, 2016.
[21] N. Sun, T. Yang, Y. Fang, B. Lu, and Y. Qian, "Nonlinear motion control of underactuated three-dimensional boom cranes with hardware experiments," *IEEE Trans. Ind. Informat.*, vol. 14, no. 3, pp. 887–897, Mar. 2018.
[22] N. Sun, Y. Fang, H. Chen, Y. Fu, and B. Lu, "Nonlinear stabilizing control for ship-mounted cranes with ship roll and heave movements: Design, analysis, and experiments," *IEEE Trans. Syst., Man, Cybern., Syst.*, to be published.
[23] S. P. Bhat and D. S. Bernstein, "Finite-time stability of continuous autonomous systems," *SIAM J. Control Optim.*, vol. 38, no. 3, pp. 751–766, Jan. 2000.
[24] L. Dai, B. Qi, H. Zhou, and K.-L. Qin, "PID control and experiment for magnetism levitation movement system," *Mod. Manuf. Eng.*, vol. 28, no. 6, pp. 79–82, Jun. 2008.
[25] Y. Sun, W. Li, D. Dong, X. Mei, and H. Qiang, "Dynamics analysis and active control of a floating crane," *Tech. Gazette*, vol. 22, no. 6, pp. 1383–1391, Dec. 2015.
[26] Y. Sun, W. Li, J. Xu, H. Qiang, and C. Chen, "Nonlinear dynamic modeling and fuzzy sliding-mode controlling of electromagnetic levitation system of low-speed MagLev train," *J. Vibroeng.*, vol. 19, no. 1, pp. 328–342, Feb. 2017.
[27] H. Wu, X.-H. Zeng, and Y. Yu, "Motion stability of high-speed MagLev systems in consideration of aerodynamic effects: A study of a single magnetic suspension system," *Acta Mech. Sinica*, vol. 33, no. 6, pp. 1084–1094, Dec. 2018.
[28] J. Li, G. Deng, C. Luo, Q. Lin, Q. Yan, and Z. Ming, "A hybrid path planning method in unmanned air/ground vehicle (UAV/UGV) cooperative systems," *IEEE Trans. Veh. Technol.*, vol. 65, no. 12, pp. 9585–9596, Dec. 2016.
[29] K. Cui and T. T. Zhao, "Unsaturated dynamic constitutive model under cyclic loading," *Cluster Comput.*, vol. 20, no. 4, pp. 2869–2879, 2017.
[30] K. Cui and X. Qin, "Virtual reality research of the dynamic characteristics of soft soil under metro vibration loads based on BP neural networks," *Neural Comput. Appl.*, vol. 29, no. 5, pp. 1233–1242, 2017, doi: 10.1007/.s00521-017-2853-7.
[31] A. Yang *et al.*, "Optimum surface roughness prediction for titanium alloy by adopting response surface methodology," *Results Phys.*, vol. 7, pp. 1046–1050, 2017.
[32] K. Cui, W.-H. Yang, and H. Gou, "Experimental research and finite element analysis on the dynamic characteristics of concrete steel bridges with multi-cracks," *J. Vibroeng.*, vol. 19, no. 6, pp. 4198–4209, 2017.
[33] K. Yang, J. Yang, J. Wu, C. Xing, and Y. Zhou, "Performance analysis of DF cooperative diversity system with OSTBC over spatially correlated Nakagami-*m* fading channels," *IEEE Trans. Veh. Technol.*, vol. 63, no. 3, pp. 1270–1281, Mar. 2014.
[34] G. Ding, Z. Tan, J. Wu, J. Zeng, and L. Zhang, "Indoor fingerprinting localization and tracking system using particle swarm optimization and Kalman filter," *IEICE Trans. Commun.*, vol. 98, no. 3, pp. 502–514, Mar. 2015.

JUNQI XU received the bachelor's degree in automation from Lanzhou Jiaotong University, Lanzhou, China, in 2000, and the master's degree in power electronics and power transmission from Southwest Jiaotong University, Chengdu, China, in 2003, where he is currently pursuing the Ph.D. degree. He is also with the National Maglev Transportation Engineering R&D Center, Tongji University, Shanghai, China. His research interests include the levitation control technology of maglev trains and coupling vibrations between maglev train and the track.

YOUGANG SUN was born in Jiangsu, China, in 1989. He received the B.S. degree in material formation and control engineering from Soochow University, China, in 2011, the M.S. degree (Hons.) in mechatronics engineering from Shanghai Maritime University, China, in 2013, and the Ph.D. degree in mechatronics engineering from Tongji University, China, in 2017. His current research interests include the aspects of dynamic systems and non-linear control.

DINGGANG GAO received the degree in mechanical engineering and automation and the master's degree in vehicle engineering from Southwest Jiaotong University, Chengdu, China, in 2000 and 2006, respectively, where he is currently pursuing the Ph.D. degree. He is also with the National Maglev Transportation Engineering R&D Center, Tongji University, Shanghai, China. His research interests include maglev vehicle technology and vehicle system dynamics.

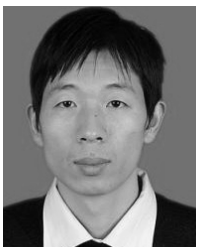

WEIHUA MA received the B.Sc. degree in vehicle engineering from Shandong University, Jinan, China, in 2002, and the Ph.D. degree in vehicle engineering from Southwest Jiaotong University, Chengdu, China, in 2008. Then, he completed the Post-Doctoral Fellowship at Southwest Jiaotong University and CRRC Qishuyan Company Ltd., in 2015. He is currently with the Traction Power State Key Laboratory, Southwest Jiaotong University. His research interests include locomotive and heavy haul train dynamics, maglev levitation frame design, and vehicle dynamics.

SHIHUI LUO was born in 1964. He received the Ph.D. degree from Shanghai Jiaotong University (SWJTU) in 1991. He is currently with SWJTU, where he is involved in railway vehicles. His research activities are focused on rail vehicle dynamics.

QINGQUAN QIAN received the B.S. degree in electrical engineering from Tangshan Jiaotong University, Tangshan, China, in 1960. He is currently a Professor of electrical engineering with Southwest Jiaotong University, Chengdu. He is a member of the Chinese Academy of Engineering. His research focuses on the analysis, operation, and design of traction power control systems.